韓國水資源學會論文集
第32卷 第1號 · 1999年 2月
pp. 83~94

사면에 발달하는 하층밀도류의 이차원흐름

Bidirectional Spreading of Gravity Underflows on an Incline

최 성 욱*
Choi, Sung-Uk

Abstract

In continental margins, turbid underflows which are not confined to a given channel, are free to spread laterally as well as longitudinally. Lateral spreading can reduce substantially the run out distance of flows along continental shelves and slopes. Laboratory experiments with a large tank, employing saline density currents as surrogates for fine-grained turbidity flows, coupled with dimensional analysis, have been used to develop a simple expression for lateral spreading rates of two-dimensional flows on sloping beds. Characteristic length and time are determined by the flow discharge and buoyancy flux at the inlet. By knowing the initial width of the flow, the spreading law can be used to estimate the maximum width of the current at different times as well as the longitudinal spreading rate. Predictions for flows compare favorably against observations.

keywords: spreading law, turbidity current, density current

요 지

대륙붕에서 부유사 하층밀도류는 양측이 수로에 제한을 받지 않기 때문에 주흐름방향인 종방향뿐만 아니라 횡방향으로도 자유롭게 흐른다. 횡방향흐름은 대륙붕 및 대륙붕사면을 따라 흐르는 밀도류의 종방향 도달거리를 크게 감축시킬 수 있다. 본 연구에서는 부유사 밀도류 대신에 염수를 이용한 밀도류 실험을 대형 탱크를 이용하여 실시하였고, 차원해석을 통하여 사면에서 밀도류의 흐름률에 관한 간단한 식을 개발하였다. 특성길이 및 특성시간은 유입부에서의 유량과 부력흐름률의 함수로 나타내었다. 유입부의 폭이 주어질 경우, 개발된 흐름식을 사용하여 시간에 따른 밀도류의 최대폭과 종방향으로의 전파속도를 계산할 수 있다. 식에 의한 예측값과 관측값이 서로 잘 일치함을 보였다.

핵심용어 : 흐름법칙, 부유사 밀도류, 밀도류

* 연세대학교 사회환경 · 건축공학부, 조교수
Assistant Professor, School of Civil, Urban, and Architectural Engineering, Yonsei University, Seoul 120-749, Korea

1. INTRODUCTION

Density currents are stratified flows caused by density differences between fluids. The reduced gravitation associated with density difference provides density currents with the driving force of propagating in the downslope direction. Thus another name of density currents is the gravity current.

Density currents may be heavier or lighter than the ambient fluids. It depends on the density relative to the surrounding fluids. Temperature, dissolved chemicals, and suspended materials induce density difference. Dense underflows are generated when the fluid heavier than the ambient fluid is released on a slope. Examples are CO_2 currents, brines from desalination plants, and turbidity currents. Of interests are turbidity currents, sediment- laden density currents. They occur in ocean, lakes, and reservoirs. Turbidity currents obtain negative buoyancy from suspended sediment. In fact, the suspended particles are so fine and continuously distributed through the dense water that they increase the density just as effectively as a dissolved substance would. However, the buoyancy of turbidity currents is not conserved because of the settling effect of particles within the current and the sediment entraining capacity of the current.

Turbidity currents move downslope carrying sediment through a submerged river or a submarine canyon. After traveling the deep-sea channel, the turbidity current arrives to a delta or a submarine fan. Then, it starts to spread laterally and shows a two-dimensional spreading pattern. At this point, the lateral spreading becomes important because it retards the longitudinal spreading rate. It has been observed that the role of the vertical spreading due to the water entrainment is insignificant for non-channelized currents compared to the lateral spreading (Fietz and Wood, 1967 ; Alavian, 1986), which enables us to take the complicated three-dimensional spreading as two-dimensional motion. Of importance is also the depositional pattern induced by the sediment-laden currents, which is relevant to both reservoir and ocean sedimentations.

Predicting the behavior of dense underflows is important in assessing the impact to such environment as rivers, lakes, and oceans. In general, for laterally-confined density currents, the front motion is described by either densimetric Froude number (Keulegan, 1957 ; Middleton, 1966 ; Benjamin, 1968 ; Kersey and Hsu, 1976 ; Kao, 1977 ; Huppert and Simpson, 1980 ; Hay, 1983 ; Altinakar et al., 1990 ; Buhler et al., 1991) or dimensionless front velocity (Britter and Linden, 1980). The densimetric Froude number presents the front velocity in terms of an appropriate length scale such as the current thickness and the reduced gravitational acceleration. Whereas the dimensionless front velocity expresses the front velocity as a function of the buoyancy flux per unit width, which is constant for buoyancy-conserving density currents. However, for non-channelized turbidity currents, which are no longer confined to a channel, a degree of freedom increases due to the lateral spreading in addition to the longitudinal spreading.

Experiments of density or turbidity currents spreading two-dimensionally, require a large-size flume especially if turbulent flows need to be generated. Mostly saline currents are substituted in the laboratory as surrogates for fine-grained sediment-laden flows. There are a couple of reasons why turbulent flows are of interest in the present study. Specifically, most of the density currents observed in ocean, lakes, and reservoirs are turbulent flows. The other reason becomes obvious when it comes to turbidity currents. In a turbidity current, the particles are suspended because of the turbulence kinetic energy. An extra source of

buoyancy can also be supplied from the bed, which is made possible by the near-bed turbulence intensity generated by the flow itself (Parker et al., 1986).

Not many previous studies are found on two-dimensional behavior of dense underflows. Alavian (1986) presented a set of differential equations for steady-state density currents, which includes the width change as a function of longitudinal distance. Alavian also showed that the spreading rate in the lateral direction is three times larger than that of the thickening rate at the normal state. Alendal et al. (1994) proposed an integral model to simulate a deep-sea gravity currents, where they made an assumption that the lateral spreading rate is the same as the thickening rate due to water entrainment. Experimental researches include Fietz and Wood (1967), Tsang and Wood (1968), Luthi (1981), Hauenstein and Dracos (1984), Alavian (1986), Tsihrintzis (1988), and Christodoulou and Tzachou (1994). It seems that the previous experiments tend to describe the behavior of gravity currents on a slope qualitatively rather than quantitatively perhaps due to the complexity of spreading mechanism.

In this paper, relationships describing the two-dimensionally spreading density currents are developed by using the dimensional analysis. Laboratory experiments are carried out to generate density currents spreading two-dimensionally on an inclined plane. Comparisons are made between the observed and predicted values from the proposed relationships.

2. LABORATORY EXPERIMENTS

2.1 Experimental Conditions

Essentially, the experiments were performed for the verification of finite element code developed to simulate two-dimensionally spreading turbidity currents. Emphasis was made on observing the bulk behavior of density currents instead of emphasizing the details of the underflow vertical structure. In the present study, however, the data from the same experiment is used to develop a relationship describing the two-dimensional flow of density current in a deep ambient water.

A wooden flume, 8 ft wide, 12 ft long, and 4 ft deep, was built in the Hydrosystems Laboratory at the University of Illinois at Urbana-Champaign. The schematic of the experimental facility is given in Fig. 1, and a picture of the constructed flume is shown in Fig. 2. A constant depth of clear water was maintained by using a morning glory type weir at the downstream end of the flume. The bottom of the inlet box was placed at a depth of 1 m, thus resulting the fractional depth of 0.1 at least. This was intended to prevent any dynamic effect from the overlying fluid layer. Therefore, no retardation in the propagation due to the relatively shallow depth near the inlet was expected.

The sloping floor was made of fiberglass, the roughness of which was found to be less smooth than the surface of glass or Plexiglass. Since the sloping part was attached to the flume with a hinge, the angle of the floor could be adjusted from 0° to 10° in the longitudinal direction. 10 cm×10 cm square grids were marked on the surface of the incline in order to monitor the two-dimensional spreading of the density current as a function of time. Fig. 3 shows a density current propagating on a sloping floor.

The contaminant tank was 4.3 ft (130 cm) wide, 5.6 ft (170 cm) long, and 5 ft (150 cm) deep. This tank was equipped with propellors which can be used to mix contaminants such as salt or sediment with the water. In order to measure the discharge of the contaminant fluid,

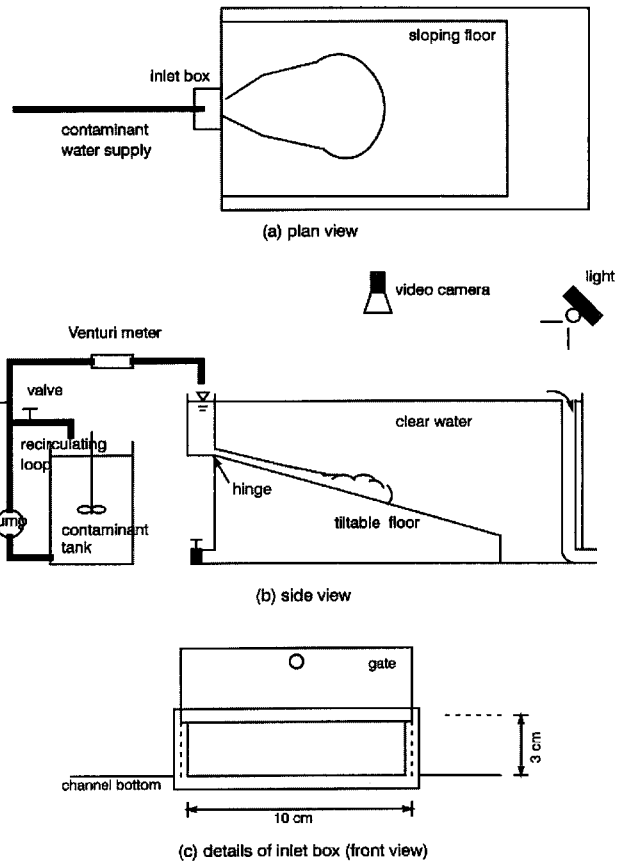

Fig. 1. Schematic of Experimental Facility (not to scale)

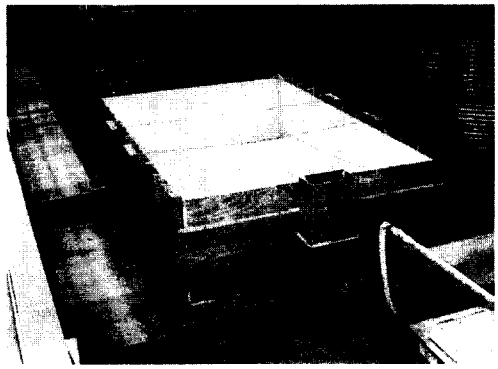

Fig. 2. Three-Dimensional Flume

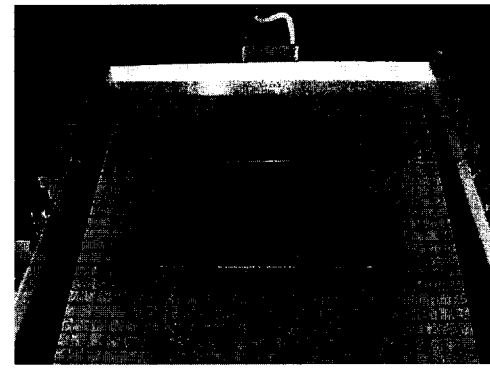

Fig. 3. Density Current Propagating on a Sloping Floor

a Venturi meter was located downstream of the pump as depicted in Fig. 1. The distance from the pump was chosen to be long enough to reduce the error due to the fluctuations of the fluid right after the pump.

Since the density currents were made visible with the help of the dye, their motion was

recorded with a video camera (Yashica, Model KD-H 170), which samples at a rate of 30 Hz. The video camera was located at the top of the crane servicing the Hydrosystems Laboratory. The spreading distances in both directions are obtained by monitoring the location of the current edge in a freezed frame with the help of the grid on the incline floor. The spreading pattern at a certain time was obtained by using a Macintosh computer equipped with a frame grabber and image analysis software (NIH Image, version 1.44). The location of the current edge was digitized with the help of the image analysis software and was saved for further analysis.

Table 1 summarizes experimental conditions and initial flow parameters at the inlet. Basically, density currents with three different buoyancy fluxes (2455, 4910, and 9820 cm^4/s^3) were generated on three different slopes (2, 5, and 10°) from DEN1 to DEN9. Different buoyancy fluxes were made by varying the fractional density which is defined by the density difference divided by the density of the ambient fluid. The width of the inlet was b_o = 10 cm except for DEN11 where b_o = 5 cm to meet the same buoyancy flux. The underflow discharge was either 500 or 1000 cm^3/s. DEN10 was executed to compare between two density currents which have the same buoyancy flux but have different inlet velocity. For all the density currents, the Reynolds number was either 4000 or 8000 and the Richardson number ranged between 0.013 and 0.212, so all the generated flows were turbulent and supercritical.

2.2 Characteristic Scales

For density currents propagating on a sloped surface, the curve of longitudinal spreading distance versus time consists of two parts; an initial transient part followed by a steady part. That is, the density current propagates in the longitudinal direction quite rapidly at the initial stage, and then propagates at an almost constant rate. This is very similar to the behavior of laterally-confined one-dimensional density currents observed in the laboratory experiments. However, for two-dimensional spreading, the longitudinal propagation rate can not be thought independently because it is extremely related with the lateral spreading. Therefore, in order to verify the longitudinal spreading rate, the lateral spreading should be considered together.

In general, the presentation of data in dimensionless form provides a more

Table 1. Summary of Experimental Data

	slope(°)	$Q_o(cm^3/s)$	Δ_o	$B_{Fo}(cm^4/s^3)$	Re_o	Ri_o
DEN1	2	500	0.005	2455	4000	0.053
DEN2	2	500	0.01	4910	4000	0.106
DEN3	2	500	0.02	9820	4000	0.212
DEN4	5	500	0.005	2455	4000	0.053
DEN5	5	500	0.01	4910	4000	0.106
DEN6	5	500	0.02	9820	4000	0.212
DEN7	10	500	0.005	2455	4000	0.053
DEN8	10	500	0.01	4910	4000	0.106
DEN9	10	500	0.02	9820	4000	0.212
DEN10	5	1000	0.005	4910	8000	0.013
DEN11*	5	500	0.01	4910	8000	0.026

* Gate width (b_o) of all experiments is 10 cm except DEN11 where b_o = 5 cm.

comprehensive interpretation of the experimental results. When the initial momentum flux (M_o) and the initial buoyancy flux (B_{Fo}) are chosen as characteristic dimensional variables, the characteristic length and time can be expressed, respectively, by (Fischer et al., 1979 ; Chu and Jirka, 1987)

$$l_j = \frac{M_o^{3/4}}{B_{Fo}^{1/2}} \tag{1}$$

$$t_j = \frac{M_o}{B_{Fo}} \tag{2}$$

The length scale by Eq. (1) represents a rough measure of longitudinal distance of the more jet-like zone, and the time scale by Eq. (2) represents a measure of time to achieve this condition. Another set of the characteristic length and time can be obtained by considering the initial volume flux (Q_o) and the initial buoyancy flux (B_{Fo}) as characteristic dimensional variables. That is, from the dimensional analysis, the characteristic length and time are found, respectively, as

$$l_p = \frac{Q_O^{3/5}}{B_{Fo}^{1/5}} \tag{3}$$

$$t_p = \frac{Q_O^{4/5}}{B_{Fo}^{3/5}} \tag{4}$$

The above variables can be successfully used to correlate the experimental data especially when the plume displays a strong plume-like behavior (Chu and Jirka, 1987 ; Baddour et al., 1980). In the present study, l_p and t_p from Eq. (3) and Eq. (4), respectively, are used as characteristic variables to make spreading distance and time dimensionless, which led better collapse of data compared to l_j and t_j from Eq. (1) and Eq. (2), respectively. Table 2 summarizes the characteristic length and time scales from the experimental conditions in Table 1. In general, the larger the ratio between the inertial force and the buoyancy force, the greater the value of both the length and time scales. The characteristic scales from Eq. (1) and Eq. (2) appear to be greater than the scales from Eq. (3) and Eq. (4). For all the experiments, the time to reach an equilibrium between the buoyancy and the momentum force does not exceed 7 s and the distance does not go beyond 35 cm. Therefore, one can conclude that the density currents generated in the present experiment reach buoyancy-dominated conditions quite quickly after being started.

2.3 Development of Spreading Law

Water entrainment through the interface plays two roles: entraining ambient water into dense water body and retarding the density current propagation. In the two-dimensional propagation of density currents, mixing takes place not only through the entrainment from upper ambient water but also through the lateral spreading. Alavian (1986) and

Table 2. Characteristic Length and Time

	l_M from eq.(1) (cm)	t_M from eq.(2) (sec)	l_* from eq.(3) (cm)	t_* from eq.(4) (sec)
DEN1, 4, 7	17.6	3.4	8.7	1.3
DEN2, 5, 8	12.4	1.7	7.6	0.9
DEN3, 6, 9	8.8	0.9	6.6	0.6
DEN10	35.2	6.8	11.5	1.5
DEN11	20.9	3.4	7.6	0.9

Tsihrintzis (1988) showed that the lateral spreading rate is three times larger than the thickening rate due to water entrainment at the normal state. Fietz and Wood (1967) observed that the vertical spreading due to mixing was observed to be small compared with the lateral spreading in the experiment with turbulent density currents. Thus, the lateral spreading seems to be more important in determining the longitudinal spreading rate of density currents than the vertical mixing.

For density plumes developing on an inclined surface, Hauenstein and Dracos (1984) proposed the following relationships under the similarity assumption:

$$u_f^{-3} \propto x, \qquad u_f^{-4} \propto t \tag{5}$$

$$b \propto x, \qquad b^{4/3} \propto t \tag{6}$$

where t denotes the time after release, x and b are the maximum travel distances in the longitudinal and lateral directions, respectively, and u_f is the front velocity in the longitudinal direction. The similarity solutions, Eqs. (5) and (6), predict that the longitudinal distance and the maximum width are directly proportional to $t^{3/4}$ for the two-dimensional spreading of density currents. However, these similarity solutions were derived under the crude assumption that the unsteady part of the spreading density current is followed by the steady-state flow, and the similarity assumption has been proved to be invalid theoretically by Safaie (1979).

Using the present experimental data, the time exponents are estimated, and the values are plotted with the bottom slope in Fig. 4. The time exponents, obtained from the best fit of the observed data, are not consistent with the slope as seen in the figure. It is found that the time exponents approach 3/4 for higher slopes. As the slope decreases, the time exponents for both the longitudinal and the lateral spreadings deviate further from the constant.

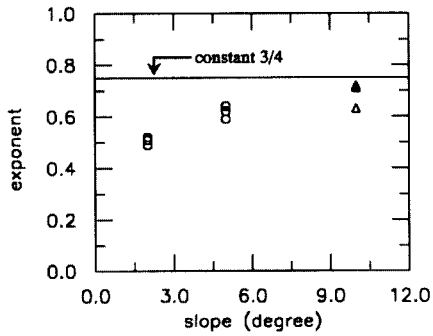

(a) For Longitudinal Spreading

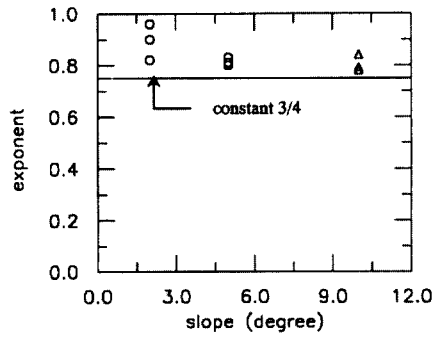

(b) For Lateral Spreading

Fig. 4. Time Exponents in Similarity Solution by Hauenstein and Dracos (1984)

The failure of the similarity solutions when applied to the present experimental results motivated the development of a relationship for the two-dimensional spreading of density currents. If the relationship is to be developed, it should be capable of describing the propagation in both directions. One constraint should be that the relationship for the two-dimensional spreading should reduce to the one-dimensional relationship if there is no lateral spreading.

Following Britter and Linden (1980), the dimensional analysis leads to the following expression for the longitudinal spreading rate:

$$u_f = c\left(\frac{B_{F_o}}{b}\right)^{1/3} f(\theta, Re) \tag{7}$$

where c is a constant. Note that the maximum width of the density current, b, is used as a characteristic length instead of the gate width. In Eq. (7), the maximum width depends on the flow parameters at the inlet and the slope, and it varies as the density current flows downstream. When the flow is highly turbulent, the dependence of u_f on the Reynolds number can be ignored. If the impact of slope can be neglected in the two-dimensional spreading of density currents, which was shown by Choi (1996), then Eq. (7) can be rewritten as

$$u_f = c\left(\frac{B_{Fo}}{b}\right)^{1/3} \tag{8}$$

which is very similar to Britter and Linden's (1980) formula for the density current propagating in one direction. As for the constant c in Eq. (8), Britter and Linden (1980) obtained 1.5 for slopes greater than 5°. For slopes less than 5°, Choi and Garcia (1995) proposed c = 1.0 from laboratory data by Altinakar et al. (1990) and numerical experiments. Note that Eq. (8) becomes the same relationship as Britter and Linden's (1980) when the width of the density current is constant in the downstream direction.

Eq. (8) is not closed because the maximum width, b, is not a determined parameter. The maximum width varies as the density current evolves with time. Herein, a collapse of the lateral spreading data is used to derive a relationship for the growth of the maximum width with respect to time. Eqs. (3) and (4) are used to make the maximum half width and the time dimensionless, respectively. Fig. 5 shows dimensionless plots of the maximum half width ($b_{1/2}$) as a function of time using

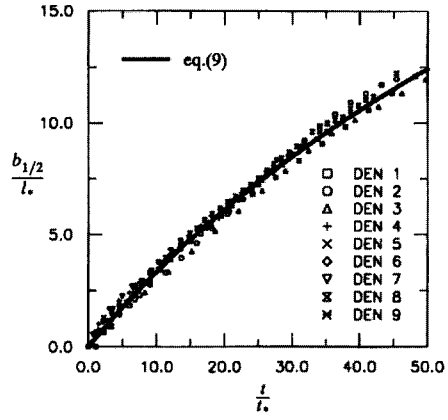

Fig. 5. Dimensionless Plot of Half Width versus Time

the data from DEN1-DEN9. A regression analysis of the data in Fig. 5 is performed to obtain a relationship between the maximum half width and time, resulting in the following expression:

$$\frac{b_{1/2}}{l_p} = 16.73 \ln\left(1 + 0.022\frac{t}{t_p}\right) \tag{9}$$

By differentiating Eq. (9), the time rate of lateral expansion of density currents can also be obtained, i.e.,

$$\frac{db_{1/2}}{dt} = \frac{l_p}{t_p}\frac{0.37}{1 + 0.022\, t/t_p} \tag{10}$$

It is seen from Eq. (10) that $db_{1/2}/dt$ is directly proportional to $(B_{Fo}^2/Q_o)^{1/5}$ and decreases as time increases. Now, if the initial width at the upstream boundary is known, the maximum width at different times is obtained by Eq. (10), which can be, in turn, used to get the longitudinal spreading rate with Eq. (8).

3. APPLICATIONS

Eq. (8) is applied to density currents propagating on the slope of 2° from data DEN1-DEN3, the results of which are given in

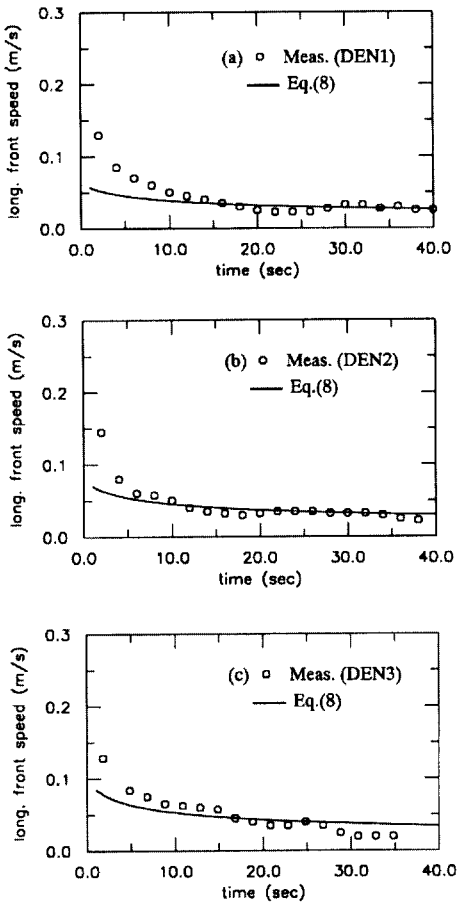

Fig. 6. Tests of Developed Relationship for Longitudinal Spreading (*for slope angle* θ = 2°)

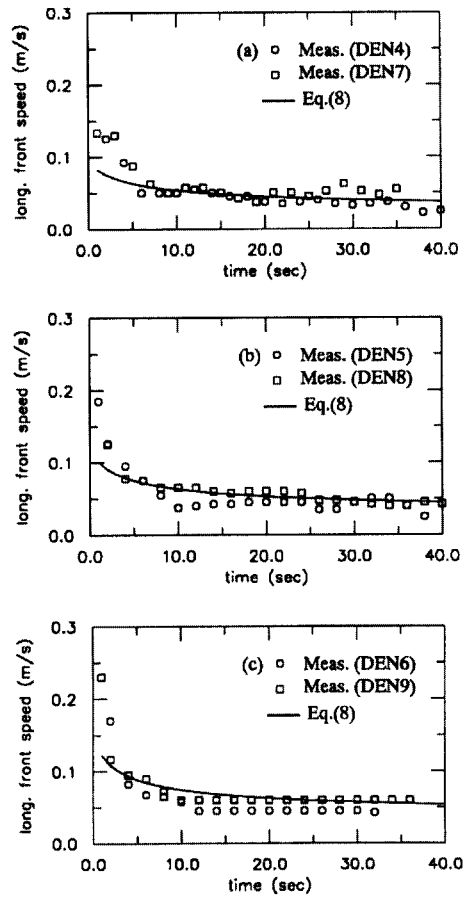

Fig. 7. Tests of Developed Relationship for Longitudinal Spreading (*for slope angle* θ > 5°)

Fig. 6. As for the constant in Eq. (8), c = 1 is used, which was proposed in Choi and Garcia (1995). Good agreement is seen between the observed and the predicted longitudinal spreading rates. The initial discrepancy between the two results is not surprising, because Eq. (8) is valid only after the density current becomes plume-like.

Fig. 7 presents the application of Eq. (8) to the density currents propagating on the slopes greater than 5° (DEN6-DEN9). The results from the measurements appear to be in fair agreement with the curve obtained from Eq. (8). Also, it is seen that the two density currents on the 5° and 10° slopes attain similar longitudinal spreading rates in the buoyancy-dominated region. This supports the fact that the impact of slope may be neglected in the longitudinal spreading once the slope exceeds 5°.

Fig. 8(a) shows an example of applying Eq. (8) to the cases of DEN5 and DEN10, which were essentially intended to investigate the effect of volume flux at the inlet. The total buoyancy fluxes (B_{Fo}) of both currents are the same, but the volume flux at the inlet

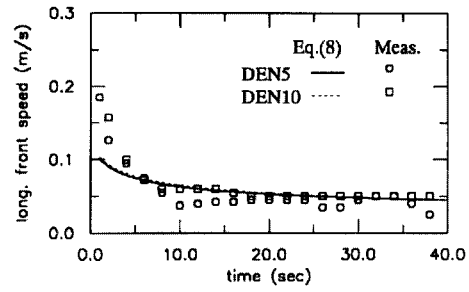

(a) Application to DEN5 and DEN10

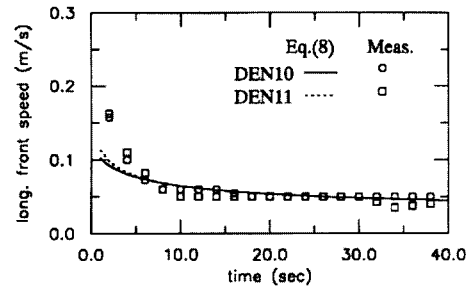

(b) Application to DEN10 and DEN11

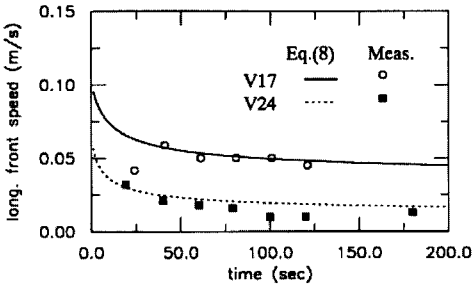

(c) Application to Hauenstein & Dracos' (1984) Data

Fig. 8. Tests of Developed Relationship for Longitudinal Spreading

(Q_o) of DEN10 is twice that of DEN5. Eq. (10) illustrates that the contribution of Q_o to $db_{1/2}/dt$ is small compared to B_{Fo}. Therefore, the difference in front spreading rates is not expected to be significant. It is interesting to note that the predictions from Eq. (8) for the two density currents are almost identical, and coincide well with the observed data. This also indicates that the volume flux at the inlet does not significantly affect the longitudinal propagating rate of density currents in the buoyancy-dominated region. The next test applies Eq. (8) to DEN10 and DEN11, and the results are given in Fig. 8(b). The total buoyancy flux (B_{Fo}) of both currents is the same, but the gate width (b_o) of DEN10 is twice that of DEN5. The two results appear to reach nearly the same speed, and also agree well with the curves obtained from Eq. (8). In Fig. 8(c), Eq. (8) is applied to the experimental data in Hauenstein and Dracos (1984). Both density currents, V17 (Q_o = 650 cm^3/s and B_{Fo} = 15380 cm^4/s^3) and V24 (Q_o = 270 cm^3/s and B_{Fo} = 419 cm^4/s^3) were generated on the 5° slope. Good agreement between the observed and the predicted propagation rates is also seen in the figure.

4. CONCLUSIONS

New relationships were developed to describe density currents propagating on an inclined slope in two directions. The longitudinal spreading rate is expressed in terms of the total buoyancy flux and the maximum width of a density current by using the dimensional analysis. The time rate of the change in the maximum width of the current, which varies along the downstream distance, was obtained from the similarity collapse of experimental data. The formulas were tested by comparing computed values with observed values. Results were found to be very promising. Impacts of the slope, volume flux, and gate width were also investigated.

REFERENCES

Alavian, V. (1986). "Behavior of density currents on an incline." *Journal of Hydraulic Engineering*, ASCE, Vol. 112, No. 1, pp. 27-42.

Alendal, G., Drange, H., and Haugan, P.M. (1994). "Modelling of deep-sea gravity currents using an integrated plume model."

The Polar Oceans and Their Role in Shaping the Global Environment, 237-246, Geophysical Monograph 85, American Geophysical Union, Washington D.C.

Altinakar, S., Graf, W.H., and Hopfinger, E.J. (1990). "Weakly depositing turbidity current on a small slope." *Journal of Hydraulic Research*, Vol. 28, No. 1, pp. 55-80.

Baddour, R.E., Ferraro, V., and Chu, V.H. (1980). "Three-dimensional underflows discharges." *Proceedings of the Second International IAHR Symposium on Stratified Flows*, IAHR, Trondheim, Norway.

Benjamin, T.B. (1968). "Gravity currents and related phenomena." *Journal of Fluid Mechanics*, Vol. 31, pp. 209-248.

Britter, R.E., and Linden, P.F. (1980). "The motion of the front of gravity current travelling down an incline." *Journal of Fluid Mechanics*, Vol. 99, pp. 531-543.

Buhler, J., Wright, S.J., and Kim, Y. (1991). "Gravity currents advancing into a coflowing fluid." *Journal of Hydraulic Research*, Vol. 29, No. 2, pp. 243-257.

Choi, S.-U., and Garcia, M. (1995). "Modeling of one-dimensional turbidity currents with a dissipative-Galerkin finite element method." *Journal of Hydraulic Research*, Vol. 30, No. 5, pp. 623-648.

Choi, S.-U. (1996). "Layer-averaged modeling of turbidity currents with a finite element method." Ph.D. thesis, Department of Civil Engineering, University of Illinois, Urbana, IL.

Christodoulou, G.C., and Tzachou, F.E. (1994). "Experiments on 3-d turbulent density currents." *Fourth International Symposium on Stratified Flows*, Proceedings of the Conference, Grenoble, France.

Chu, V.H., and Jirka, G.H. (1987). "Surface buoyant jets and plumes." *Encyclopedia of Fluid Mechanics*, edited by N.P. Cheremisinoff, Vol. 6, Chapter 25, pp. 1053-1084.

Fietz, T.R., and Wood, I.R. (1967). "Three-dimensional density current." *Journal of The Hydraulics Division*, ASCE, Vol. 93, No. HY6, pp. 1-23.

Fischer, H.B., List, E.J., Koh, R.C.Y., Imberger, J., and Brooks, N.H. (1979). *Mixing in Inland and Coastal Waters*. Academic Press, London, United Kingdom.

Hauenstein, W., and Dracos, T.H. (1984). "Investigation of plunging density currents generated by inflows in lake." *Journal of Hydraulic Research*, Vol. 22, pp. 157-179.

Hay, A.E. (1983). "On the frontal speeds of internal gravity surges on sloping boundaries." *Journal of Geophysical Research*, Vol. 88, No. c1, pp. 751-754.

Huppert, H.E., and Simpson, J.E. (1980). "The slumping of gravity currents." *Journal of Fluid Mechanics*, Vol. 99, pp. 785-799.

Kao, T.W. (1977). "Density currents and their applications." *Journal of The Hydraulics Division*, ASCE, Vol. 103, No. HY5, pp. 543-555.

Kersey, D.G., and Hsu, K.J. (1976). "Energy relations of density current flows: an experimental investigation." *Sedimentology*, Vol. 23, pp. 761-789.

Keulegan, G.H. (1957). "Thirteenth progress report on model laws for density currents. An experimental study of the motion of saline water from locks into fresh water channels." *U.S. National Bureau of Standards Report*, 5168.

Luthi, S. (1981). "Experiments on non-channelized turbidity currents and their deposits." *Marine Geology*, Vol. 40, M59-M68.

Middleton, G.V. (1966). "Experiments on density and turbidity currents. I. Motion of the head." *Canadian Journal of Earth Sciences*, Vol. 3, pp. 523-546.

Parker, G., Fukushima, Y., and Pantin, H.M. (1986). "Self accelerating turbidity currents." *Journal of Fluid Mechanics*, Vol. 171, pp. 145-181.

Safaie, B. (1979). "Mixing of buoyant surface jet over sloping bottom." *Journal of the Waterway Port Coastal and Ocean Division*, ASCE, Vol. 105, No. WW4, pp. 357-373.

Tsang, G., and Wood, I.R. (1968). "Motion of two-dimensional starting plume." *Journal of the Engineering Mechanics Division*, Vol. 94, No. EM6, pp. 1547-1561.

Tsihrintzis, V.A. (1988). "Theoretical and experimental investigation of three-dimensional boundary-attached density currents." Ph.D. thesis, Department of Civil Engineering, University of Illinois, Urbana, IL.

APPENDIX. NOTATIONS

The following symbols are used in this paper:

b = width of density current ;

$b_{1/2}$ = half width of density current ;

b_o = inlet width ;

b_F = total buoyancy flux ($= g\Delta Q$) ;

l_j = characteristic length in jet region ;

l_p = characteristic length in plume region ;

o = subscript denoting the inlet site ;

Q = volume flux or discharge ;

Re = Reynolds number ;

Ri = bulk Richardson number ;

t = time ;

t_j = characteristic time in jet region ;

t_p = characteristic time in plume region ;

u_f = front speed in the longitudinal direction ;

x = longitudinal distance ;

Δ = fractional density of density current ($= \Delta\rho/\rho$) ; and

θ = slope angle (in degree).

(논문번호:98-071/접수:1998.11.12/심사완료:1999.01.06)